Energy & Environmental Science

Accepted Manuscript

ROYAL SOCIETY OF CHEMISTRY

www.rsc.org/ees

Energy & Environmental Science

Cite this: DOI: 10.1039/c0xx00000x

www.rsc.org/ees

COMMUNICATION

Encapsulating V_2O_5 into Carbon Nanotube Enables Flexible High-Performance Lithium Ion Batteries

Debin Kong,[a,b] Xianglong Li,[b] Yunbo Zhang,[b] Xiao Hai,[b] Bin Wang,[b] Xiongying Qiu,[b] Qi Song,[b] Quan-Hong Yang[a]* and Linjie Zhi[a,b]*

Received (in XXX, XXX) XthXXXXXXXXX 20XX, Accepted Xth XXXXXXXXX 20XX

DOI: 10.1039/b000000x

Here, we have designed and successfully fabricated an interwoven nanocable architecture constructed by V_2O_5 nanosheets encapsulated with multi-graphitic nanotubes as a novel high performance flexible cathode for Li ion batteries. Such an integrated electrode designed via the multiscale system exhibits ultrafast and stable Li ion storage performance, with a capacity higher than 90 mAh g^{-1} even at 100 C and only 0.04% capacity decay per cycle over 200 cycles. To the best of our knowledge, this is the first example for the facile synthesis of flexible V_2O_5 encapsulated in carbon nanotube positive electrodes and the successful demonstration of a flexible full cell showing surprisingly consistent cycling stability and excellent mechanical properties with V_2O_5@G as cathodes and their allotrope as anodes. Remarkably, an energy density of ca. 360 Wh kg^{-1} at a power rate of 15.2 kW kg^{-1} is achieved, which belongs to one of the best results reported so far on V_2O_5-based electrode materials. Coupled with a simple and scalable production protocol, the strategies is highly promising for both novel cathode exploring and the practical fabrication and application of flexible energy storage devices.

Rechargeable batteries with high energy density and good flexibility are urgently required in many applications nowadays, ranging from portable electronic devices to electric vehicles. Unfortunately, the commercial lithium ion batteries (LIBs) so far cannot satisfy these requirements simultaneously.[1-6] To improve the performance of LIBs, great efforts have been devoted to developing new electrode materials, designing novel electrode structures, and decreasing inactive ingredients in the electrodes. However, currently, the most-studied materials for particularly positive-electrode can only reversibly accept one electron and deliver capacities lower than 200 mAh g^{-1} in general.[7, 8] On the other hand, the fabrication of flexible energy storage devices for next-generation, flexible and wearable electronic devices with high-performance still faces big challenges.[9, 10] Accordingly, great attention has been paid to the exploration of new battery systems with mechanical flexibility and high energy density.

Vanadium pentoxide, V_2O_5, is believed to be a good host for reversible Li^+ insertion/extraction according to the simplified reactions originated from its layered crystal structure along the c-axis.[11] More attractively, it can capture multiple electrons during the reaction and thus enables a high theoretical capacity of 294 mAh g^{-1} in the voltage range of 4.0−2.0 V (vs Li/Li^+).[12, 13] Unfortunately, up to now, V_2O_5 experiences degradation upon lithium ion diffusion and holds poor conductivity, which results in rapid capacity fading and poor rate capability.[14-16] To address these problems, diverse V_2O_5-based cathodes have been fabricated and exploited, including three-dimensional (3D) porous electrodes with a conductive backbone,[17] nanometer-scale architectures with short ion/electron transportation paths,[18-20] and/or conductive layer coating on active materials[21]. However, the V_2O_5 used in these cases is normally in powder form and thus needs to be mixed with extra additives (e.g., carbon black), polymer binders or metal substrates, which decrease significantly the energy and power density of the whole electrodes. Recently, Fan *et al.*[8] pioneered the deposition of a V_2O_5 nanobelt array directly on graphene foam, which was then used as a binder-free cathode, resulting in a cell with excellent electrochemical performance although the V_2O_5 content of the cathode is limited to less than 60% due to the selected synthesis procedure. Moreover, compared to the in-situ synthesis procedure, the ex-situ synthesis procedure with step-by-step growing of V_2O_5 on various substrates as reported in most of the literatures may suffer a less effective interfacial interaction between V_2O_5 and the substrate and the growth on the substrate results in the detachment of the active materials and the generation of large particles during cycling due to the lack of the restriction. From the view point of further developing V_2O_5-based flexible energy storage devices, a binder-free V_2O_5-based electrode with good mechanical properties and excellent flexibility is required as well, which is another big challenge in this field.

In this communication, as schematically shown in **Figure 1a** and **b**, we have developed a novel in-situ strategy and successfully fabricated a unique 1D composite structure through the encapsulation of V_2O_5 nanoparticles into a carbon nanotube

via the combination of electrospinning technique with chemical vapor deposition (CVD) methods. The CVD grown graphitic carbon are rolling up into hollow carbon nanotubes and the in-situ formed V_2O_5 nanosheets are uniformly encapsulated into the nanotubes, thus forming mechanically robust, V_2O_5@G nanocables which are further interwoven into free-standing and flexible webs. More interestingly, due to the excellent flexibility and the free standing nature, such integrated V_2O_5@G based electrodes can be directly used as cathodes for the fabrication of flexible lithium ion batteries, which exhibit ultrafast and stable Li ion storage performance, with a reversible capacity of 224 mAh g^{-1} at 0.1 C and a capacity higher than 90 mAh g^{-1} even at a large current density of 30 A g^{-1} (100 C) and retained a stable cyclic performance with 0.04% capacity decay per cycle even over 200 cycles. To the best of our knowledge, this is the first example for the facile synthesis of flexible V_2O_5-based positive electrodes and the successful demonstration of a flexible full cell showing surprisingly consistent cycling stability and excellent mechanical properties with V_2O_5@G as cathodes and their allotrope (flexible SnO_x-encapsualted carbon nanotube network) as anodes.

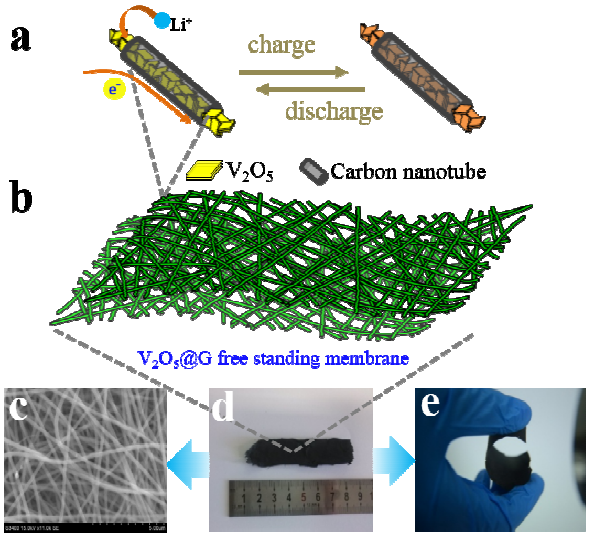

Figure 1 Electrode design and fabrication. (a) Schematic diagram of a single nanocable where V_2O_5 uniformly encapsulated into the graphitic nanotube. (b) Schematic of the configuration of self-supported flexible V_2O_5@G membrane interwoven by nanocables. (c) SEM images of V_2O_5@G membrane. (d and e) Photographs showing of self-supported flexible V_2O_5@G membrane under flat and bent states.

The fabrication of V_2O_5@G mainly involves electrospinning of polyvinyl pyrrolidone solution containing vanadium source and tetraethylorthosilicate followed by a CVD process. As exhibited in **Figure 1d, e**, the resultant V_2O_5@G assemblies are mechanically robust and free-standing, showing a significantly improved electrical conductivity of 0.7 S cm^{-1} (**Figure S1**) as well as mechanical strength (**Figure S2**). This characteristic enables their direct use as LIB electrodes without introducing any supplementary components and further as the electrodes of flexible batteries. Besides, the size of the film obtained depends on the size of the container. In our experiment, one batch of the prepared sample can easily reach 3 cm × 8 cm, which indicates the feasibility for scale up production **(Figure 1d)**. The zoomed scanning electron microscopy (SEM) images of the film (**Figure 1b and c**) clearly indicate that the thus-fabricated hybrid web is composed of interconnected nanowires and each nanowire is around 150 nm in diameter and several micrometers in length (**Figure 1d**). To further zoom in each nanowire (**Figure 1a**), the cable wall consists of few layered graphitic carbon where the V_2O_5 are evenly embedded in a single nanocable. In our case, the uniform dispersion characteristics of spinning solution makes each component, such as vanadium, uniformly dispersed in the obtained nanowires (**Figure S3**). Through in situ decomposition of methane, few layers of graphitic carbon are deposited on the surface of obtained nanofibers. The introduced graphitic carbon coating is suggested to be vital for maintaining the mechanical robustness and electric connectivity of the web. As shown in **Figure S3**, graphitic carbon layers are grown on the surface of silica nanofiber through CVD process to form nanotubes. Notably, similar to the results reported previously by other research groups, graphitic carbon coatings grown on silica substrate are not structurally perfect but multi-crystalline, defect-containing layers.[22, 23] Actually, these characters of structure imperfections and defects are critically important for providing multiple pathways for efficient lithium ion transportation.[24, 25]

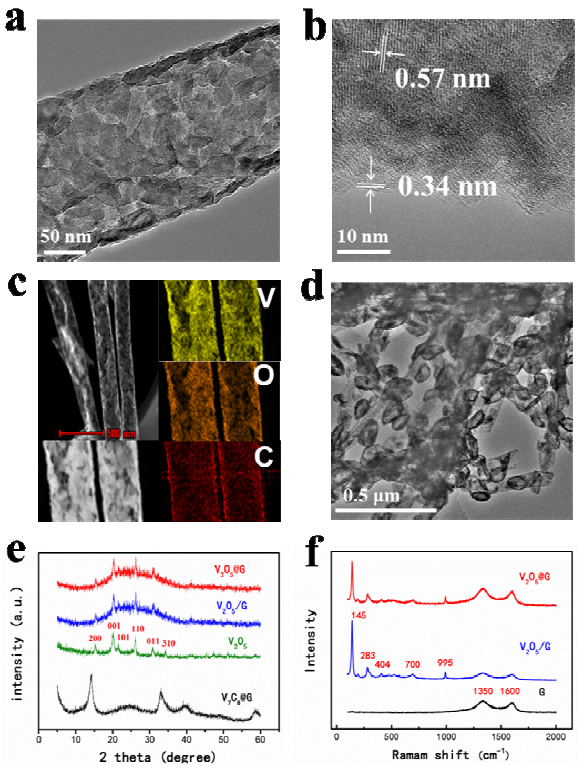

Figure 2 Microstructure and composition analysis. (a) TEM image of V_2O_5@G. Scale bar, 50 nm. (b) High-magnification TEM images of V_2O_5@G. Scale bar, 10 nm. (c) Vanadium, Oxygen and Carbon elemental mapping of a selected area of an individual V_2O_5@G. Scale bar, 500 nm. (d) TEM image of V_2O_5/G.Scale bar, 0.5 μm; (e) XRD patterns of these samples: V_2O_5@G and V_2O_5/G and intermediate product V_7C_8@G. (f) Raman pattern of V_2O_5@G and V_2O_5/G

The detailed microstructure of the obtained sample was analyzed using transmission electron microscopy (TEM) and high-resolution TEM (HRTEM). The TEM images further demonstrate the nanostructure of each nanocable, wherein the cable wall consists of few layered graphitic carbon (average thickness: 5 nm) and the V_2O_5 are evenly embedded in a single nanocable (**Figure 2a, b**). The characteristic lattice fringe corresponding to 0.57 nm and 0.34 nm in the high resolution TEM images of V_2O_5@G should be attributed to the interplanar distance of V_2O_5 and the (002) lattice of multilayer graphitic carbon, respectively.[26] Besides, the energy dispersal X-ray spectroscopy (EDS) mapping results of V, O and C elements further proves this hetero nanocable structure where ultrathin V_2O_5 distribute evenly in the entire nanocable for V_2O_5@G (**Figure 2c**). As a comparison, a reference sample, V_2O_5/G, is prepared by ex-situ synthesis, in which the V_2O_5 is formed via hydrothermal method with the addition of vanadium source after CVD process. Compared to V_2O_5@G, V_2O_5/G hold a similar V content as well as similar nanocables network but a quite different character in which V_2O_5 are in the outer wall of the graphitic nanotubes (**Figure 2d, Figure S4**).

More evidence about the phase and composition of the products are provided by the X-ray diffraction (XRD), Raman, and X-ray photoelectron spectroscopy (XPS) results. As shown in **Figure 2e** with the peaks labeled, which demonstrates that all the reflections of the samples are in good agreement with the standard pattern of pure orthorhombic V_2O_5 phase (JCPDS card no. 89-0612).[27] For the Raman spectra, both samples show similar patterns as exhibited in **Figure 2f**. In addition to the typical peaks of graphitic carbon (D peak at around 1350 cm^{-1} and G peak at around 1600 cm^{-1}), the peaks at 284, 306, 406, 483, 525,702, and 996 cm^{-1}, which are characteristic modes for V_2O_5.[28] Besides, the chemical compositions of the composites confirm the expected carbon at 284.5 eV, vanadium at 517.1 eV, and oxygen at 530.1 eV by XPS (**Figure S5**). The binding energy of vanadium and oxygen as determined in XPS indicates the formation of V-oxides in the composites.[29]

To evaluate the electrochemical properties of the V_2O_5@G nanocable webs, two-electrode coin-type cells (2032) with metallic lithium counter electrodes have been fabricated using V_2O_5@G and V_2O_5/G as cathode, respectively, and with no other additives. **Figure 3a** shows typical cyclic voltammetry (CV) curves at a scan rate of 0.1 mV s^{-1}. It can be seen the CV behavior is generally consistent with that of V_2O_5 reported previously. The first reduction peak at ca. 3.4 V is due to the conversion of α-V_2O_5 into ε-$Li_{0.5}V_2O_5$. Then reductions take place at ca. 3.2 V and ca. 2.3 V, corresponding to the formation of δ-LiV_2O_5 and γ-$Li_2V_2O_5$, respectively. These reactions are reversible and contribute to a large capacity of the electrode. Further reduction corresponds to the formation of the irreversible ω-$Li_xV_2O_5$ (x > 2) phase, which is detrimental to the cyclic capacity retention.[4, 30]

More attractive result is that when V_2O_5@G is used as a binder-free cathode of LIBs, a high reversible capacity of about 224 mAh g^{-1} is achieved in the initial cycles at 0.15 A g^{-1} (0.5 C). Considering that the content of V_2O_5 in the nanocable is 75wt% as confirmed by TGA (**Figure S6**), a calculated specific capacity on pure V_2O_5 is ca. 298 mAh g^{-1}, which is very close to the theoretical capacity of V_2O_5 for two lithium intercalations (294 mAh g^{-1}). Coulombic efficiency is calculated to be 92.4% at the first cycle, which is related to the irreversible replacement of protons and formation of some solid–electrolyte interface.[31,32] Interestingly, even after 200 cycles, both the discharge and charge capacities of this material are stable at about 211 mAh g^{-1}, delivering 91.7% capacity retention. The excellent cycling stability of V_2O_5@G can be mainly ascribed to the improved electric conductivity and the high structural stability of graphitic carbon-based nanocables network. In comparison, V_2O_5/G revealed a relatively poor cycling stability (only 73.9% capacity retention after 200 cycles), as shown in **Figure 3b**. Considering that the only difference between the two samples is that the V_2O_5 is deposited in the inner wall of graphitic nanotube for V_2O_5@G while in the outer wall for V_2O_5/G, the capacity decay on V_2O_5/G probably arises from the exfoliation of the active substrate and the generation of large particles during cycling due to the lack of the restriction from the tube wall, which influences both the

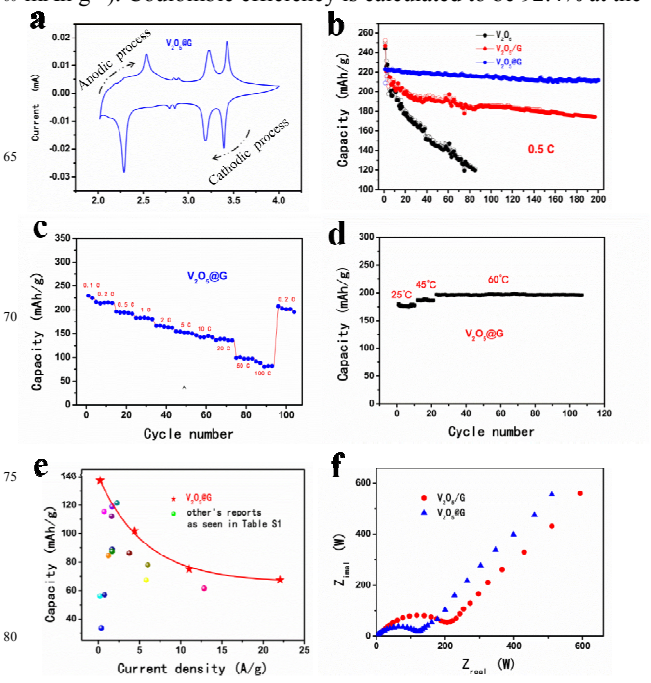

Figure 3 Electrochemical characteristics of half cell. (a) Representative CVs at a scan rate of 0.1 mV s^{-1} for the first cycles of V_2O_5@G. (b) Different cycle performance of V_2O_5@G, V_2O_5/G and pure V_2O_5 electrodes at current density of 0.5C. (c) Reversible capacity of V_2O_5@G at various current rates from 0.1 C to 100 C. (d) the electrochemical performances of the V_2O_5@G architectures at current density of 1 C at various selected temperatures, 25 °C, 45 °C, and 60 °C. All the capacities reported are on the basis of the whole electrode. (e) Comparison of the current density and capacity based on the total mass of the whole electrode of the V_2O_5@G electrode with that of V_2O_5-based batteries from some recent publications. (f) Nyquist curve of electrochemical impedance measurements (EIS) of V_2O_5@G and V_2O_5/G.

formation of conductive networks and the diffusion dynamics of the lithium ions, suggesting an important role of the carbon nanotube coating on the cycling ability (cycling performance with different thickness of carbon coating as shown in **Figure S7**). As shown in **Figure S8**, the unique nanocable architecture of V_2O_5@G can be well maintained even after 100 cycles, while micro-scale particles are observed on V_2O_5/G.

In order to achieve high power densities for practical applications, such as the commercial production of electric vehicles, the rate performance of LIBs is another critically important concern. **Figure 3c** shows the rate capability of V_2O_5@G. Excitingly, the hybrid nanocables V_2O_5@G deliver an outstanding rate performance, revealing a reversible capacity of 224 mAh g^{-1} at a current density of 0.03 A g^{-1} (0.1 C) in the first cycle, and a capacity of around 90 mAh g^{-1} even when the current density increases to 30 A g^{-1} (100 C) (the corresponding full charge or discharge time is only 36 s). When the current density decreases to 0.06 A g^{-1} (0.2 C) after cycling under high current densities, V_2O_5@G can still regain a reversible capacity of ca. 220 mAh g^{-1}.

In the case of cathode materials with excellent high-rate performances, the electrochemical performance at high temperatures is also very important for practical batteries. Thus, we investigated the electrochemical behaviors of the V_2O_5@G electrode at various selected temperatures, such as 25 °C, 45 °C and 60 °C. As shown in **Figure 3d**, on increasing the environmental temperature from 25 to 60 °C, the reversible capacity clearly increases from 200 to 220 mAh g^{-1} at a current rate of 1 C. The capacity increase should be attributed to the significantly enhanced diffusion rates of lithium ions in the electrodes at higher temperatures. Moreover, the V_2O_5@G architecture exhibits a quite stable cycling performance even at high temperatures.

It's worth noting that such an excellent electrochemical performance as mentioned above is achieved on the basis of the whole electrode, free of any auxiliary components (e.g., binder, conductive carbon, foils), which will significantly increase the capacity for the final device in comparison to conventional LIBs. The Ragone plot in **Figure 3e** illustrates the performance of our electrodes (the total mass of the positive electrode was used for the calculation of energy and power densities).To the best of our knowledge, such an outstanding performance has never been reported previously on V_2O_5-based electrode materials, which means that the herein developed novel V_2O_5@G is among the most promising cathode materials for lithium ion storage and for high power Li-ion batteries (**Table S1**). Besides, because of the judicious material and structure design, our V_2O_5@G electrode indeed shows the merits of both LIB and supercapacitors. For example, an energy density of ca. 360 Wh kg^{-1} at a power rate of 15.2 kW kg^{-1} is achieved, which is much higher than V_2O_5 related materials previously reported. These high-rate values are even much higher than those reported on aqueous-system supercapacitors (usually lower than 60 Wh kg^{-1}). The comparison in **Figure 3f** unambiguously demonstrates that the unique V_2O_5@G electrodes indeed have an outstanding performance in terms of both energy and power densities.

To further understand the enhanced performance of V_2O_5@G architecture, we conducted EIS tests on V_2O_5@G and V_2O_5/G to reveal their electrochemical reaction kinetics. As shown in **Figure S6**, three samples all show a semicircle in high to medium frequency regions and an inclined line in low frequency regions, which correspond to the electrochemical reaction impedance (namely, charge transfer) and the ion diffusion impedance, respectively.[33] The much smaller diameter of the semicircle for V_2O_5@G in the high–medium frequency region indicates the greatly decreased charge-transfer resistance at the electrode/electrolyte interface, which is resulted from the sufficient contact between the electrolyte and the uniformly distributed active V_2O_5 due to the restriction from tube wall during cycling.

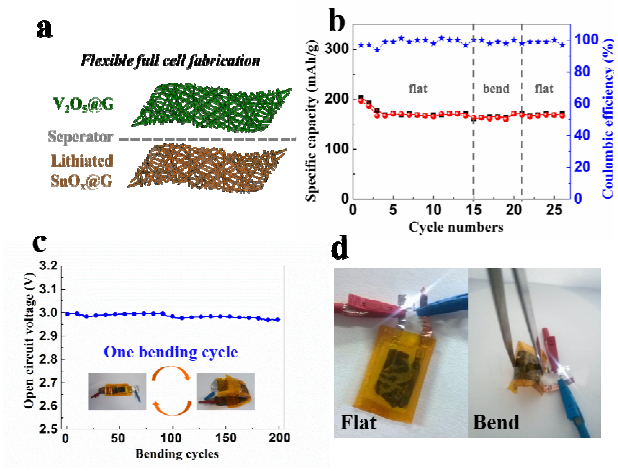

Figure 4 Electrochemical characteristics and flexiblity of full cell. (a) The scheme of fabrication of a flexible prototype Sn-V_2O_5 battery. (b) The cycle performance of the full cell at current density of 0.5 C. (c) Stability of full cell to resist bending. The open circuit voltage over 200 bending cycles. (d) Photographs of a prototype flexible Sn-V_2O_5 lighting a white LED device under flat and bent states.

The excellent performance of our designed V_2O_5@G nanocables with both high energy density and high power density could be attributed to harmonious integration of several distinct advantages via the multiscale system (the nano-, micro- and macro-scale). Firstly, at the battery pack scale (macro-scale), the obtained free-standing and conductive film enables the construction and direct utilization without the extra weight of additives, polymer binders, and metal substrates. This scenario is quite different from previous studies on binder/conductive additive-involved V_2O_5 cathodes in which the substantial need of extra substances really dilutes the lithium ion storage performance in terms of both volumetric capacity and gravimetric capacity because the total electrode weight and volume must be considered from a practical point of view. Secondly, at the materials ensemble scale (micro-scale), the interconnection of graphitic carbon coating nanocables not only provides the most efficient 1D electron transport pathways but also forms a strong skeleton framework that can tolerate strain relaxation and accommodate the volume change of V_2O_5, which effectively

mitigates the stress and protects the active materials from pulverization during the discharge/charge process. Thirdly, at individual materials unit (nano-scale), nanoscale diameter and uniform dispersion of the V_2O_5 particles as well as the large contact area between nanocables and the electrolyte accelerate the Li-ion transport due to the shortened diffusion paths, resulting in excellent rate ability and high power density. More importantly, to our best knowledge, it is the first time for the in-situ synthesis of flexible V_2O_5-based positive electrodes and successful fabrication of a V_2O_5-based flexible energy device. The in-situ synthesis is considered more desirable than ex-situ synthesis (such as growing on various substrates) in terms of a more effective interfacial area creating robust hybrids capable of intimate charge and energy transfer.

Furthermore, in order to verify the feasibility of this flexible electrode design, we have fabricated a flexible Sn-V_2O_5 battery prototype, which is also the first V_2O_5-based flexible battery so far. This battery assembled in a glove box using the same electrolyte mentioned above shows excellent flexibility as shown in **Figure 4a and S8,** and the size can reach up to 1.5 cm × 8 cm. The V_2O_5@G positive electrode and the SnO_x@G negative electrode are laminated onto both sides of a separator using an Al foil and a Cu foil connecting with the light-emitting diode (LED) devices. The cycle stability and mechanical property of the flexible batteries were further investigated. As illustrated in **Figure 4b and c**, the capacity which is calculated based on the entire weight of V_2O_5@G mass can reach almost 200 mAh g^{-1} in the first cycle. Interestingly, after a slight decay in the first two cycles, the capacity of flexible batteries delivered over 90% capacity retention during the following cycles. More importantly, the capacity of flexible batteries remained nearly unchanged even after cycling five times at the bend state of 180 angles for 5 cycles, indicating that the flexible have excellent mechanical properties. To further verify the flexibility and mechanical properties of the flexible batteries, the inset of Figure 3c displayed how the flexible batteries were bended. Even over 200 bending cycles, the open circuit voltage remained at 3V stably and can still drive a white LED no matter it is flat or bent (**Figure 4d)**.

In conclusion, we have designed and successfully fabricated a novel cathode material for the fabrication of flexible Li ion batteries. The unique cathode is a flexible web film composed of V_2O_5@G nanocables in which the V_2O_5 nanoparticles are encapsulated into a carbon nanotube. The as fabricated battery cell exhibits not only excellent flexibility but ultrafast and stable Li ion storage performance, with a reversible capacity of 224 mAh g^{-1} at 0.1 C and a capacity higher than 90 mAh g^{-1} even at an ultrahigh charging rate of 100 C, maintaining a quite stable cyclic performance with only 0.04% capacity decay per cycle even over 200 cycles. Remarkably, an energy density of ca. 360 Wh kg^{-1} at a power rate of 15.2 kW kg^{-1} is achieved based on the electrode materials. To the best of our knowledge, it is the first time for the facile synthesis of flexible V_2O_5 encapsulated in carbon nanotube positive electrodes as well as the successful fabrication of a V_2O_5-based flexible energy storage device showing surprisingly good cycling stability and excellent mechanical properties. Coupled with a simple and scalable production protocol, the strategies developed in this work is highly promising for both novel cathode exploring and the practical fabrication and application of flexible energy storage devices.

Notes and references

[a] *School of Chemical Engineering and Technology, Tianjin University, Tianjin, 300072 (China)*
[b] *CAS Key Laboratory of Nanosystem and Hierarchical Fabrication, CAS Center for Excellence in Nanoscience, National Center for Nanoscience and Technology, Beijing 100190, China*
E-mail: zhilj@nanoctr.cn, qhyangcn@tju.edu.cn

† Electronic Supplementary Information (ESI) available. See DOI: 10.1039/b000000x/

£The authors acknowledge the support from the Ministry of Science and Technology of China (No.2012CB933403), the National Natural Science Foundation of China (Grant No. 21173057, 51425302), and the Chinese Academy of Sciences.

1. B. Kang and G. Ceder, *Nature*, 2009, **458**, 190-193.
2. Y. Wang and G. Cao, *Adv. Mater.*, 2008, **20**, 2251-2269.
3. P. G. Bruce, S. A. Freunberger, L. J. Hardwick and J.-M. Tarascon, *Nat. Mater.*, 2012, **11**, 19-29.
4. M. Lee, S. K. Balasingam, H. Y. Jeong, W. G. Hong, B. H. Kim and Y. Jun, *Sci. Rep.*, 2015, **5**, 8151.
5. A. Pan, H. B. Wu, L. Yu and X. W. Lou, *Angew. Chem. Int. Ed.*, 2013, **125**, 2226–2230.
6. H. Liu and W. Yang, *Energy Environ. Sci.*, 2011, **4**, 4000-4008.
7. J.-M. Tarascon and M. Armand, *Nature*, 2001, **414**, 359-367.
8. D. Chao, X. Xia, J. Liu, Z. Fan, C. F. Ng, J. Lin, H. Zhang, Z. X. Shen and H. J. Fan, *Adv. Mater.*, 2014, **26**, 5794-5800.
9. G. Jeong, Y.-U. Kim, H. Kim, Y.-J. Kim and H.-J. Sohn, *Energy Environ. Sci.*, 2011, **4**, 1986-2002.
10. S.-Y. Lee, K.-H. Choi, W.-S. Choi, Y. H. Kwon, H.-R. Jung, H.-C. Shin and J. Y. Kim, *Energy Environ. Sci.*, 2013, **6**, 2414-2423.
11. Y. L. Cheah, V. Aravindan and S. Madhavi, *J. Electrochem. Soc.*, 2013, **160**, A1016-A1024.
12. Y. Tang, X. Rui, Y. Zhang, T. M. Lim, Z. Dong, H. H. Hng, X. Chen, Q. Yan and Z. Chen, *J. Mater. Chem. A*, 2013, **1**, 82-88.
13. A. Pan, H. B. Wu, L. Yu and X. W. D. Lou, *Angew. Chem. Int. Ed.*, 2013, **125**, 2282-2286.
14. J. Liu, H. Xia, D. Xue and L. Lu, *J. Am. Chem. Soc.*, 2009, **131**, 12086-12087.
15. X. Rui, J. Zhu, W. Liu, H. Tan, D. Sim, C. Xu, H. Zhang, J. Ma, H. H. Hng and T. M. Lim, *RSC Adv.*, 2011, **1**, 117-122.
16. L. Mai, F. Dong, X. Xu, Y. Luo, Q. An, Y. Zhao, J. Pan and J. Yang, *Nano Lett.*, 2013, **13**, 740-745.
17. Y. Huang, J. Liang and Y. Chen, *Small*, 2012, **8**, 1805-1834.
18. B. Saravanakumar, K. K. Purushothaman and G. Muralidharan, *ACS Appl. Mater. Interfaces*, 2012, **4**, 4484-4490.
19. P. G. Bruce, B. Scrosati and J. M. Tarascon, *Angew. Chem. Int. Ed.*, 2008, **47**, 2930-2946.
20. A. S. Arico, P. Bruce, B. Scrosati, J.-M. Tarascon and W. Van Schalkwijk, *Nat. Mater.*, 2005, **4**, 366-377.
21. X.-F. Zhang, K.-X. Wang, X. Wei and J.-S. Chen, *Chem. Mater.*, 2011, **23**, 5290-5292.
22. J. Chen, Y. Wen, Y. Guo, B. Wu, L. Huang, Y. Xue, D. Geng, D. Wang, G. Yu and Y. Liu, *J. Am. Chem. Soc.*, 2011, **133**, 17548-17551.
23. B. Wang, X. Li, T. Qiu, B. Luo, J. Ning, J. Li, X. Zhang, M. Liang and L. Zhi, *Nano Lett.*, 2013, **13**, 5578-5584.
24. D. Kong, H. He, Q. Song, B. Wang, W. Lv, Q.-H. Yang and L. Zhi, *Energy Environ. Sci.*, 2014, **7**, 3320-3325.
25. X. Li, Q. Song, L. Hao and L. Zhi, *Small*, 2014, **10**, 2122-2135.
26. H. B. Wu, A. Pan, H. H. Hng and X. W. Lou, *Adv. Func. Mater.*, 2013, **23**, 5669-5674.

27. Y. Dong, H. Wei, W. Liu, Q. Liu, W. Zhang and Y. Yang, *J. Power Sources*, 2015, **285**, 538-542.
28. M. Li, G. Sun, P. Yin, C. Ruan and K. Ai, *ACS Appl. Mater. Interfaces*, 2013, **5**, 11462-11470.
29. Y. Yang, L. Li, H. Fei, Z. Peng, G. Ruan and J. M. Tour, *ACS Appl. Mater. Interfaces*, 2014, **6**, 9590-9594.
30. Q. An, P. Zhang, F. Xiong, Q. Wei, J. Sheng, Q. Wang and L. Mai, *Nano Res.*, 2015, **8**, 481-490.
31. X. Jia, Z. Chen, A. Suwarnasarn, L. Rice, X. Wang, H. Sohn, Q. Zhang, B. M. Wu, F. Wei and Y. Lu, *Energy Environ. Sci.*, 2012, **5**, 6845-6849.
32. W. J. H. Borghols, D. Lützenkirchen-Hecht, U. Haake, W. Chan, U. Lafont, E. M. Kelder, E. R. H. van Eck, A. P. M. Kentgens, F. M. Mulder and M. Wagemaker, *J. Electrochem. Soc.*, 2010, **157**, A582-A588.
33. Y. Gong, S. Yang, Z. Liu, L. Ma, R. Vajtai and P. M. Ajayan, *Adv. Mater.*, 2013, **25**, 3979-3984.

TOC

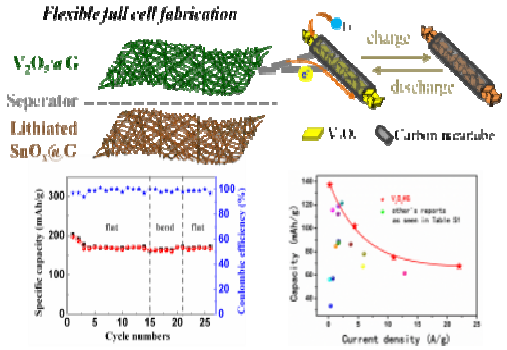

A facile synthesis of high performance flexible V_2O_5-based cathodes constructed by V_2O_5 nanosheets encapsulated with multi-graphene nanotubes and the successful demonstration of a flexible full cell.

Broader Context

Interface interaction of graphene-based hybrid materials is critically important for enhancing their electrochemical properties in energy storage devices. Molybdenum sulfide has received great attention as an anode material in lithium ion batteries due to its layered structure and high theoratical capacity up to around 669 mA h g^{-1}. However, how to incorporate it with various carbonaceous materials to successfully strike a balance between maximizing the MoS_2 content and maintaining an effective conductive network of the entire anode remains a big challenge. Herein, for the first time we have successfully designed a novel contact mode between MoS_2 and graphene, where graphene rolls up into a tubular structure and thin MoS_2 nanosheets are uniformly standing on the inner surface of the nanotube to form a unique MoS_2@graphene nanocable. Surprisingly, such a hybrid structure can maximize the MoS_2 loading for every individual nanocable in which over 90 % of MoS_2 nanosheets with stacked layer number of less than 5 can be installed. When been used as a binder-free electrode, this mechanically robust, unique nanocable film not only shows excellent cycling performance (almost 100% capacity retention even after 160 cycles) but exhibits a surprisingly high-rate capability of 900 mA h g^{-1} even at 5 A g^{-1}, which is one of the best results reported so far on MoS_2-based electrode materials. This newly developed 2D@2D designing strategy opens up a new window as well for rational fabrication of various 2D building block-based hybrid materials for applications in energy storage, electrocatalysis, opto-electronics and many other fields.